Effect of Activation Temperature on Properties of H₃PO₄-Activated Carbon

Wei Xu, Junli Liu,* Kang Sun, Yanyan Liu, Chao Chen, Ao Wang, and Hao Sun

The effects of different activation temperatures (T_a), ranging from 300 to 750 °C, on the ash content, yield, ignition point, microcrystalline structure, surface functional group, pore structure, and adsorption performance of activated carbon in preparing activated carbon by phosphoric acid (H₃PO₄) were systematically studied. The yield and volatile content of activated carbon decreased with the increase of T_a, while the ash content, ignition point, and graphitization degree showed the opposite results. The turning point of ash content increasing rate of activated carbon occurred at 500 °C. The thermal decomposition temperature of phosphonate compounds was approximately 450 °C. With increased T_a, micropores were generated first, followed by mesopores. The ignition point of activated carbon was related to the volatile content and the degree of graphitization. Activated carbon with low ash content, high yield, well-developed pore structure and good adsorption performance was prepared at 350 to 425 °C. With increased T_a, the volatile content decreased, and the ignition point of activated carbon increased. At T_a higher than 500 °C, the aromatic and condensed ring structure, graphitization degree, and mesopore ratio of the activated carbon increased, yielding decreased adsorption performance.

Contact information: Institute of Chemical Industry of Forest Products, CAF; National Engineering Lab. for Biomass Chemical Utilization; Key Lab. of Chemical Engineering of Forest Products, National Forestry and Grassland Administration; Key Lab. of Biomass Energy and Material, Jiangsu Province; Jiangsu Co-Innovation Center of Efficient Processing and Utilization of Forest Resources, Longpan Road, Nanjing, 210042, China; *Corresponding author: liujunli1974@126.com

INTRODUCTION

Producing activated carbon from biomass waste is a good way to reduce environmental pollution and the use of limited resources (Hesas *et al*. 2014; Jain *et al*. 2016). Phosphoric acid (H₃PO₄) is used industrially for preparing activated carbon from lignocellulosic materials (Heidarinejad *et al*. 2020). H₃PO₄ is effective for producing mesopores at lower temperatures. In addition, H₃PO₄ provides an easier way to recover the carbon product during processing stage by rinsing with water (Yahya *et al*. 2015). Compared with other activating compounds such as KOH (Mao *et al*. 2015), ZnCl₂ (Duan *et al*. 2019), and K₂CO₃ (Mao *et al*. 2020), it also gives higher yield of activated carbon and has non-toxic properties (Romero-Anaya *et al*. 2012). The H₃PO₄ method has been used for almost 40 years. At present, approximately 0.2 million tons of activated carbon is produced by H₃PO₄ in China (Environmental Monitoring Center Station of Ningxia 2018). With a huge market demand, the activated carbon is an indispensable and important chemical product for the national economy and ecological environment construction.

Activation temperature (T_a) is an important factor in the preparation of H₃PO₄-activated carbon because H₃PO₄ works above 300 °C (Jagtoyen and Derbyshire 1998; Zuo

et al. 2010). The T_a affects the thermal decomposition of cellulose, hemicellulose, and lignin (Yang *et al*. 2007; Chen *et al*. 2018). Moreover, T_a affects the formation and thermal transformation of phosphonate compounds to connect and crosslink biopolymer fragments (Zuo *et al*. 2018). Finally, T_a is a direct factor for H_3PO_4 to dehydrate and polymerize itself (Kang *et al*. 2018). The influence of T_a on the surface area, pore development, and yield of activated carbon have been investigated. Increasing temperature is beneficial for the formation of pores in the carbon, especially when the temperature increases from 400 to 500 °C (Luo *et al*. 2019). This is ascribed to the use of activating agent releasing the tar from the cross-linked framework (Foo and Lee 2010). However, with further increases in temperature, violent gasification reactions destroy part of the micropore structure, leading to decreased surface area and pore volume (Chen *et al*. 2013). Moreover, increased temperature elevates the ash and fixed carbon percentage, decreasing the volatile matter and the solid yield (Ioannidou and Zabaniotou 2007). A final T_a of 400 °C is suitable for producing high-surface-area activated carbon (Yorgun and Yildiz 2015; Kang *et al*. 2018). This temperature is favorable for increasing yield and reducing ash content. Thus, the T_a is usually in the range of 400 to 500 °C (Demiral and Şamdan 2016; Villota *et al*. 2017; Villota *et al*. 2019), and the activated carbon prepared at these temperatures can have well-developed porous structure and large adsorption capacity, which is beneficial for decolorization, water purification, catalytic carriers, and other industrial needs (Malaika *et al*. 2018; Wu *et al*. 2019).

With the increasing need for special activated carbon, especially for activated carbon with low ash content, high ignition point, and controlled pore size, the existing activated carbon products no longer meet the market demand. While there have been studies on the formation of ash, the change of ignition point, and the relationship between pore development and adsorption properties of activated carbon, research on the heat treatment process is limited. Therefore, it is necessary to systematically study the influence of T_a on the properties of H_3PO_4-activated carbon. This study examined the influence of T_a on the ash content, yield, pore structure, adsorption performance, ignition point, microcrystalline structure, surface functional groups, and changes in microstructure. The results of this research can be used for reference in the preparation of special activated carbon with controllable pore structure, good adsorption, low ash content, or high ignition point.

EXPERIMENTAL

Materials

Analytical grade H_3PO_4 (85% by mass), iodine, methylene blue, and sodium thiosulfate were purchased from Aladdin Co. Ltd. (Shanghai, China). Fir sawdust (FS, 10- to 35-mesh, lignin content of 31.46%) was provided by Yuanli Active Carbon Co. Ltd. (Fujian, China). The ultimate analysis and proximate analysis of FS are listed in Table 1.

Table 1. Ultimate Analyses and Proximate Analyses of FS

Ultimate Analyses ar/wt%				Proximate Analyses ar/wt%			
C	N	H	O	ash	moisture	volatile	fixed carbon
49.73	0.29	6.65	39.6	0.74	3.27	81.20	18.06

Preparation of activated carbon

FS (50 g) was soaked with H_3PO_4 solution (55 wt%) according to the immersion ratio of 1.5:1. After stirring for 30 min, the mixture was pretreated in an oven at 140 °C for 120 min, then moved to a muffle furnace under N_2 flow and activated at 300 °C to 750 °C for 120 min. After activation, they were taken out, washed in deionized water (500 mL) for 3 times (each time for 3 min), and dried to obtain the activated carbon.

Test Standards

The ash content, iodine number, methylene blue number, ignition point, and volatile matter of activated carbon were determined as per GB/T 12496.3(1999), GB/T 12496.8 (2015), GB/T 12496.10 (1999), GB/T 12496.6 (1999), GB/T 20449 (2006), and GB/T 17664 (1999), respectively.

Methods

The BET specific surface area was measured using a Micromeritics ASAP 2460 apparatus (Norcross, GA, USA) at 77 K. The pore size distribution was computed based on the density functional theory (DFT) method. Thermogravimetric analysis (TG) was carried out by a Netzsch STA449C apparatus (Selb, Germany). A 10 mg sample was heated to 800 °C under the protection of the nitrogen with a heating rate of 10 °C/min. The X-ray diffraction (XRD) was performed on a Bruker D8 Advance X-ray diffractometer (Karlsruhe, Germany) with Cu Kα radiation (λ=0.154 nm), Scanning range was 10 to 80° with 0.1°/s. The Fourier transform infrared (FTIR) was tested on a Magna-IR spectrometer 550 (Madison, WI, USA) in the range of 4000 to 400 cm^{-1} with a resolution of 4 cm^{-1}.

RESULTS AND DISCUSSION

Effect of T_a on Ash Content and Yield of Activated Carbon

Low ash content in activated carbon is necessary when used for injection, wine, catalyst support, *etc*. In order to explore the preparation method of low ash content activated carbon, the effect of T_a on the ash content of activated carbon was studied, as shown in Fig. 1(a). The ash content of activated carbon increases with the elevation of T_a. At the T_a lower than 350 °C, activated carbon with ash content less than 2% was prepared. When the T_a ranged from 350 to 500 °C, the ash content increased slightly. When the temperature was raised from 500 to 550 °C, the ash content greatly increased from 3.54% to 6.00%. This means that the turning point of ash content increasing rate of activated carbon occurred at 500 °C. Further elevation of the T_a caused only slight changes in the ash content of activated carbon. The results indicated that the T_a should be lower than 500 °C for preparation of low ash content activated carbon.

The influence of T_a on ash content is closely related to the polymerization of H_3PO_4 at different temperatures. With the increase of T_a, H_3PO_4 dehydrates continuously to form viscous liquid or solid such as pyrophosphoric acid, metaphosphoric acid, polyphosphoric acid, and phosphorus pentoxide (Greenwood and Earnshaw 2012; Kang *et al*. 2018), which block the pores of activated carbon. Most of these polyphosphates are recycled during activated carbon rinsing. The unremoved polyphosphate remains in the pores of activated carbon, creating an important source of ash. The rapid increase of ash content of activated carbon at 500 to 550 °C means that there was more polyphosphoric acid generated in this temperature range, and it is difficult to elute. In addition, water-insoluble phosphate was

formed *via* the reaction of H_3PO_4 and metal salts in raw materials under high temperature. The phosphonate compounds were produced by condensation of H_3PO_4 and hydroxyl groups of high glycan (include their degradation products) are also important sources of ash.
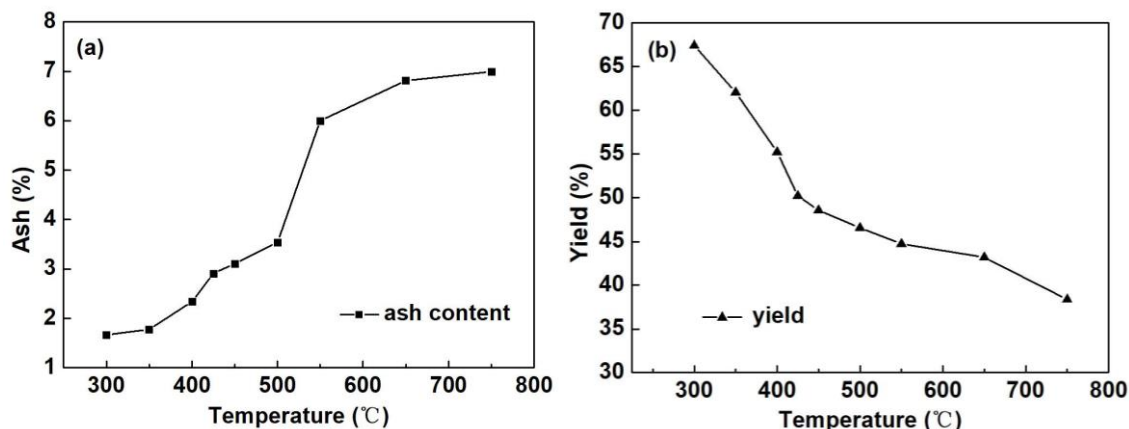

Fig. 1. (a) Ash content and (b) yield of activated carbon with different T_a

As shown in Fig. 1(b), the yield of activated carbon was affected by T_a. During the preparation of activated carbon, the yield of activated carbon continuously decreased with the increase of T_a. When T_a was 300 °C, the yield was 67.4%, and the yield decreased to 48.6% at 450 °C. The turning point of the curve occurred at 450 °C, showing that the pyrolysis rate was faster and the degree of pyrolysis was higher before 450 °C. The effect of T_a on the yield is related to the degree of pyrolysis of raw materials at different temperatures. With increasing temperature, the cellulose, hemicellulose, and lignin making up the sawdust are pyrolyzed gradually, resulting in a continually decreased yield. To compare the influence of H_3PO_4 on the pyrolysis process of sawdust, TG (Fig. 2) was carried out for FS and fir sawdust impregnated H_3PO_4 (FS-H_3PO_4). The thermal decomposition of FS was concentrated in 250 to 400 °C, and the mass loss in this range was increased from 4.28% to 71.4%. After the FS was soaked with H_3PO_4, the thermal decomposition range was changed into two stages, 130 to 450 °C (mass reduced from 91.4% to 66.9%) and 450 to 700 °C (mass reduced from 66.9% to 28.2%). Comparing the TG curves for the two specimens, the addition of H_3PO_4 improved the yield and changes the thermal decomposition process of FS (Yagmur *et al*. 2018). In the pyrolysis process, the catalytic dehydration of H_3PO_4 makes the weight loss of FS-H_3PO_4 more obvious before 334 °C. Above 334 °C, H_3PO_4 forms stable phosphonate compounds with FS, protects the pyrolysis of FS, and enhances the yield (Yakout and Eldeen 2016), whereas the pyrolysis of FS unimpregnated H_3PO_4 is more obvious. The weight drop of FS-H_3PO_4 after 450 °C can be explained by the destruction of phosphonate compounds (Solum *et al*. 1995; Jagtoyen and Derbyshire 1998) and the volatilisation of phosphorus compounds (Suarezgarcia *et al*. 2004; Puziy *et al*. 2005). It is more appropriate to assume that P_2O_5 (formed by dehydration of H_3PO_4) behaves as an oxidant, which can react with carbon, reducing the yield and forming new pores (Olivaresmarin *et al*. 2006). The mechanism of this process is shown in Fig. 3, and the result is consistent with the turning point of yield in Fig. 1(b) at 450 °C. The volatilisation of phosphorus compounds does not lead to the decrease of ash content of activated carbon, and it can be inferred that the phosphorus compounds are not the only source of ash in activated carbon.
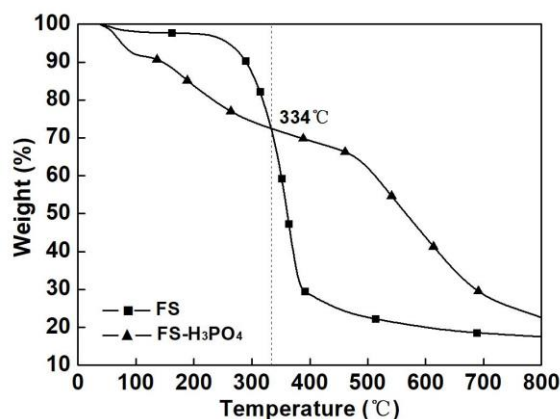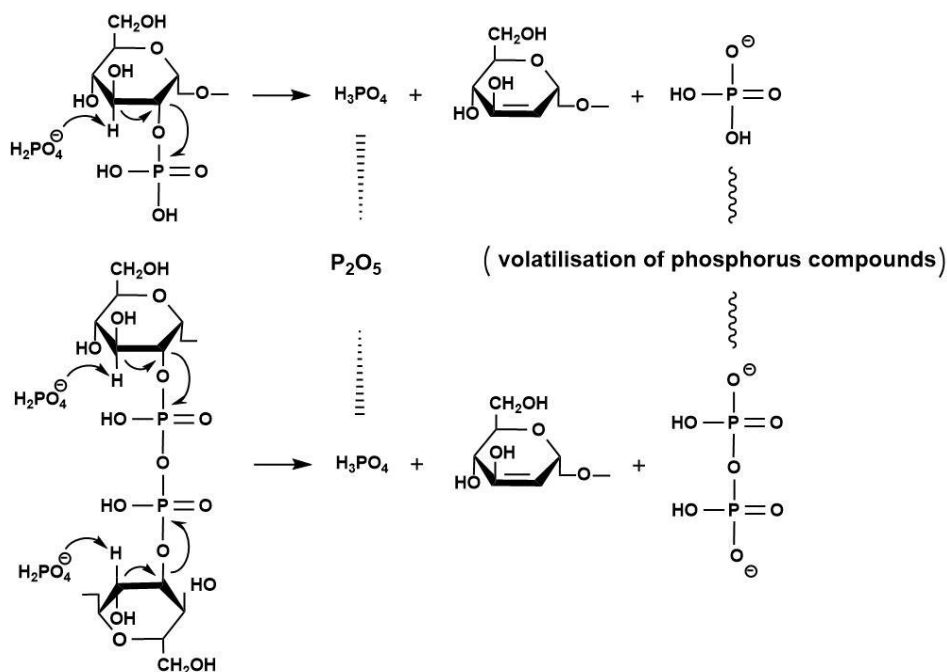
Fig. 2. TG curves of FS and FS-H$_3$PO$_4$

Fig. 3. Mechanism of phosphonate compounds decomposition (T_a > 450 °C)

Effect of T_a on Ignition Point and Volatile of Activated Carbon

The ignition point is an important index to evaluate the thermal stability of activated carbon in gas phase application. As shown in Fig. 4, the ignition point of activated carbon increased with elevated T_a. Before 450 °C, the ignition point of activated carbon was lower than 300 °C. When the T_a increased to 500 °C, the ignition point of the activated carbon exceeded 300 °C, and flame-retardant activated carbon with an ignition point greater than 400 °C was prepared at a T_a of 750 °C. The effect of T_a on the ignition point may be related to the reduction of volatile content of activated carbon. This is because CO, H$_2$, CH$_4$, and other gaseous organics from pyrolysis are conducive to the combustion of activated carbon. The relationship between the content of volatile matter and the ignition point of activated carbon was studied (Fig. 4). The volatile content of activated carbon decreased with the increased T_a, which is contrary to the change trend of ignition point with T_a. It was

concluded that the ignition point is correlated negatively to the volatile content of activated carbon. When the T_a increased from 300 °C to 425 °C, the volatile content decreased from 27.3% to 23.4%, and the volatile content decreased to 21.9% with the T_a at 750 °C. Compared with the volatile content (81.2%) of FS, the pyrolysis of FS was sufficient at 300 to 425 °C (Ferrera-Lorenzo *et al*. 2014; Li *et al*. 2015), which may be a basis for the formation of developed pore structure of activated carbon at low T_a.
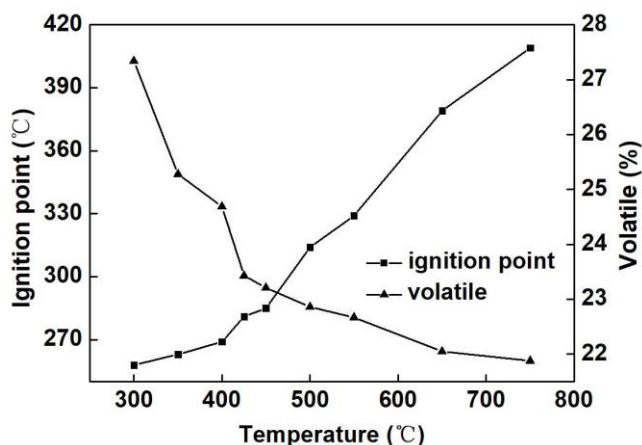

Fig. 4. Ignition point and volatile of activated carbon with different T_a

Effect of T_a on Microcrystalline Structure and Surface Functional Groups of Activated Carbon

XRD was employed to analyze the effect of different T_a on the microcrystalline structure of the activated carbon. As shown in Fig. 5a, three diffraction peaks at 16°, 22°, and 34° for FS represent the (101), (002), and (004) crystal planes of cellulose (Ma *et al*. 2017). Two obvious peaks are observable at 24° and 42° for activated carbon corresponding to the (002) and (100) planes of amorphous carbon (Chen *et al*. 2017). These changes indicate that the crystalline area of cellulose was destroyed after activation, representing the formation of amorphous carbon. The amorphous carbon produced above 300 °C is the basis for the formation of pores. The pores are produced by removing various carbon-containing compounds and disordered carbon between the basic crystallites of amorphous carbon during the preparation of activated carbon (Wigmans 1986). With the increase of T_a, the diffraction peak of amorphous carbon gradually increases and shifts to the high angles, the stacking thickness of carbon layer along (100) direction increases, and the degree of graphitization increases (Wada *et al*. 2010). The exception occurs at 650 °C and 750 °C, when the (002) shifts to low angles, which may be related to the channel collapse at high temperature. The elevated degree of graphitization makes the internal structure of activated carbon orderly and regular. The reduction of the spacing of microcrystalline layers may make the internal phosphoric acid unable to elute. The formation of stable graphite-like microcrystalline structures may also reduce their tendency to spontaneous combustion.
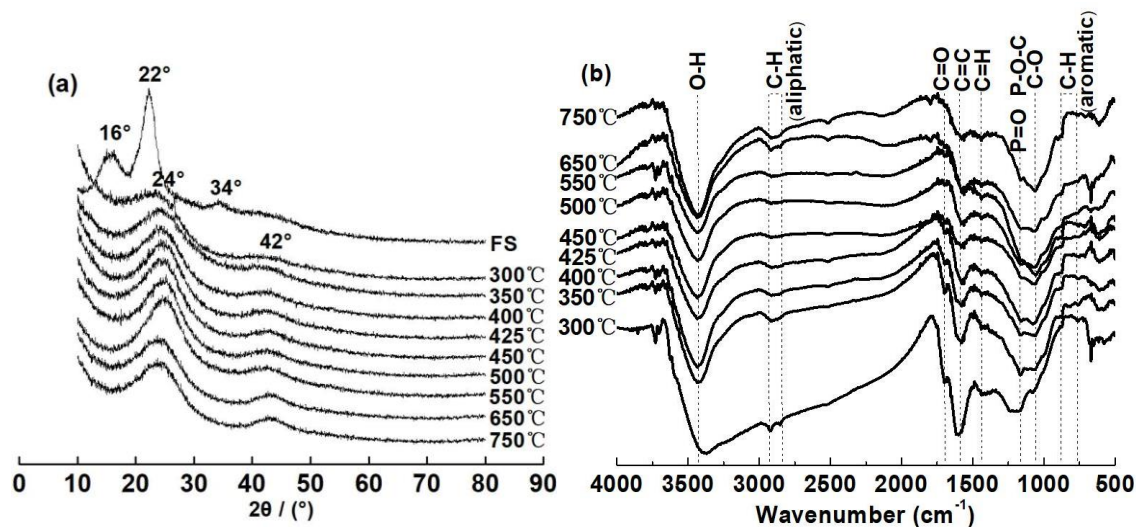
Fig. 5. (a) XRD and (b) FTIR curves of activated carbon with different T_a

The changes in functional groups on the surface of activated carbon prepared at different T_a were studied by FTIR, as shown in Fig. 5b. In all spectra, the band located at 3430 cm^{-1} can be assigned to the O-H stretching mode. The band of activated carbon prepared at 300 °C is obviously asymmetric, indicating the existence of hydrogen bond (Ma *et al*. 2017). A small peak at 2920 to 2850 cm^{-1} can be assigned to the C-H stretching mode, and its bending mode appears at 1440 cm^{-1} (Mao *et al*. 2018). The band of C=O appears at 1700 cm^{-1}. With increased T_a, the intensity of C=O decreased and disappeared above 500 °C, and the band position shifted to a low wave number, indicating decarbonylation. This effect was apparent when the intensity of C-O (1060 cm^{-1}) increased with the elevated T_a. A strong band at 1580 cm^{-1} was ascribed to the stretching vibration of aromatic ring (C=C), demonstrating that the carbonyl (1700 cm^{-1}) is conjugated with aromatic ring. A small red shift with the increase of T_a indicated the growth of aromatic ring structure (Puziy *et al*. 2002), which is unfavorable to the adsorption performance of activated carbon but is the basis for the enhancement of the structural order and graphitization degree of activated carbon (Leung and Safford 1970). The increase of aromatic ring structure is caused by the catalytic dehydration of phosphoric acid, and the process is shown in Fig. 6 (Benaddi *et al*. 1998). The band at 1160 cm^{-1} is assigned to phosphates with stretching mode of P=O, P-O-C, and P=OOH. The bands at 1060 cm^{-1} are due to C-O stretching in alcohols, phenols, ethers, and esters, or P$^+$-O$^-$ (Puziy *et al*. 2005; Ma *et al*. 2018). The broad band between 750 cm^{-1} and 900 cm^{-1} corresponding to the out-of-plane bending mode of aromatic ring C-H weakened and disappeared when T_a was higher than 500 °C. The change indicates that the functional group of activated carbon has replaced or formed a dense ring structure.
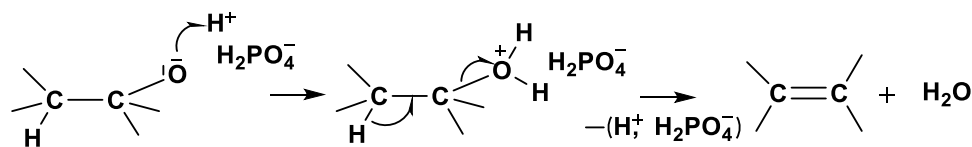

Fig. 6. Dehydration reaction of sugar molecules catalyzed by phosphoric acid

Effect of T_a on Pore Structure and Adsorption Properties of Activated Carbon

The N_2 adsorption-desorption isotherms of the activated carbon are presented in Fig. 7(a). The isotherms of activated carbon prepared at 300 °C belong to type I (Sing 1982; Rouquerol *et al*. 1994). The micropores of activated carbon were confirmed by the abundant pores and in the range of 1 to 2 nm, as can be seen in Fig. 7(b) as low V_{mes}/V_{tot} ratio and small D_{ave} value (Table 2). When the T_a is higher than 300 °C, the isotherms of activated carbon belong to type IV (Sing 1982; Rouquerol *et al*. 1994). The hysteresis loop appearing at high relative pressures ($P/P_0 > 0.4$) indicates that the mesopores of activated carbon are developed and corresponds with the large number of mesopores distributed at 2.7, 3.4, and 8.7 nm, as shown in Fig. 7(b). At the same relative pressure, the adsorption capacity of N_2 was consistent with the S_{BET} and V_{tot} of activated carbon, which is shown in Table 2. The pore structure of activated carbon prepared at different T_a was distributed in the range of 0 to 50 nm. At the same diameter, the different proportion of pores reflect the amount of V_{tot} of activated carbon prepared at different T_a.
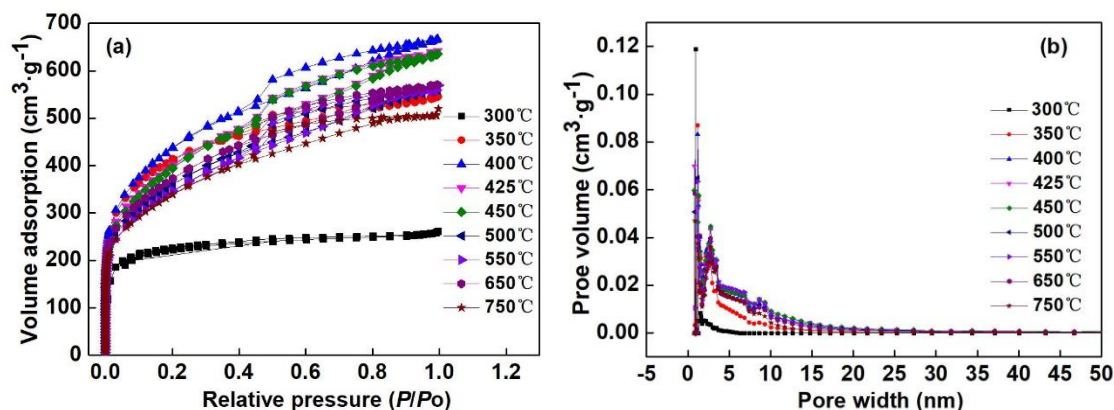

Fig. 7. (a) N_2 adsorption-desorption isotherms and (b) DFT pore size distributions of activated carbon with different T_a

The pore parameters of activated carbon based on N_2 adsorption-desorption isotherms are given in Table 2. With increasing T_a, the S_{BET} and V_{tot} of activated carbon increased first and then decreased. When the T_a is 300 °C, the pore structure of the prepared activated carbon is underdeveloped with the S_{BET} of 799 m^2/g and V_{tot} of 0.34 cm^3/g. When the T_a increased from 300 to 350 °C, the S_{BET}, V_{tot}, and V_{mes}/V_{tot} of the activated carbon increased, suggesting that the effect of H_3PO_4 is enhanced at this temperature. Increasing the T_a to 450 °C, the S_{BET} and V_{tot} were further developed and tended to be stable. At an T_a of 400 °C, the S_{BET} and V_{tot} of activated carbon reached maximum values, which were 1547 m^2/g and 0.89 cm^3/g, respectively. At the T_a between 450 to 550 °C, the S_{BET} and V_{tot} of activated carbon showed a downward trend, relating to the destruction of the phosphate bond, the ablation of the cell wall, and the collapse of the pore structure during high temperature (Romeroanaya *et al*. 2012). A slight increase of S_{BET} and V_{tot} at 650 °C is related to the rearrangement of microcrystalline structure during skeleton contraction. The increase of S_{BET} from 350 to 400 °C was not significant, but the V_{tot} and V_{mes}/V_{tot} were increased, indicating that this stage is conducive to the formation of mesopores. The V_{mes}/V_{tot} ratio of activated carbon increased with the elevation of T_a and reached the maximum at 450 °C, which can be ascribed to the formation of mesopores at the high T_a

(Jagtoyen and Derbyshire 1998). The change of V_{mes}/V_{tot} was supported by the change trend of the D_{ave}.

Table 2. Pore Parameters of Activated Carbons with Different T_a

T_a (°C)	S_{BET}(m²/g)	V_{tot}(cm³/g)	V_{mes}(cm³/g)	V_{mes}/V_{tot} (%)	D_{ave}(nm)
300	799	0.34	0.04	11.76	2.03
350	1434	0.72	0.30	41.67	2.36
400	1547	0.89	0.50	56.18	2.67
425	1421	0.86	0.51	59.30	2.79
450	1408	0.86	0.52	60.46	2.79
500	1274	0.76	0.43	56.58	2.72
550	1227	0.78	0.47	60.26	2.87
650	1285	0.77	0.43	55.84	2.68
750	1168	0.72	0.39	54.17	2.69

*S_{BET} : BET surface area, V_{tot}: Total pore volume, V_{mes} : Mesopore volume, V_{mes}/V_{tot} : Mesoporosity, D_{ave} : Average pore diameter.

Iodine number (IN) and methylene blue number (MBN) are important references for evaluating the adsorption performance of activated carbon. The influence of T_a on IN and MBN of activated carbon were studied (Fig. 8). With increased T_a, the curve of the IN showed a trend of first increasing and then decreasing. When the T_a was 450 °C, the IN reached the highest value of 834 mg/g. Further increasing the T_a to 500 °C, the IN decreases significantly. The IN of activated carbon does not change much at 500 to 750 °C. The influence of MBN on activated carbon is relatively weak by the T_a. Both low T_a (425 °C) and high T_a (650 °C) can prepare activated carbons with MBN exceeding 285 mg/g. The MBN on activated carbon prepared at 450 to 550 °C was less than 250 mg/g. The IN and MBN of activated carbon are used to measure the development of micropores and mesopores, respectively (Nunes and Guerreiro 2011; Hirunpraditkoon*et al*. 2015). When the T_a was lower than 400 °C, the IN of activated carbon was high enough. The MBN increased with the elevation of T_a from 300 to 425 °C, indicating that mesopores were generated. This result was consistent with the conclusion that pore structure was affected by T_a. At T_a higher than 500 °C, the IN and MBN of activated carbon were not regular with the collapse of old pores and the formation of new pores. Thus, activated carbon with higher IN and MBN should be prepared at a T_a between 350 and 425 °C.
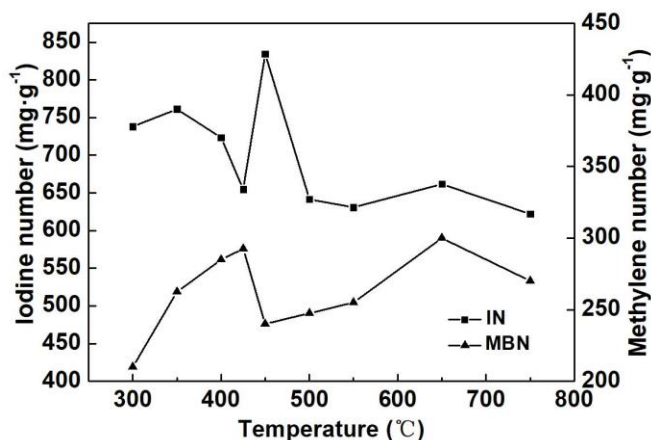

Fig. 8. IN and MBN curves of activated carbon with T_a

CONCLUSIONS

1. The activated carbon with low ash content should be prepared at an activation temperature (T_a) lower than 500 °C. This is because the turning point of ash content increasing rate of activated carbon occurs at 500 °C. The thermal decomposition temperature of phosphonate compounds about 450 °C, can be demonstrated by the weight reduction of FS-H_3PO_4. The yield curve of activated carbon turned at a T_a value higher than 450 °C.

2. The volatile content is negatively relating to the ignition point of activated carbon. At a T_a of 750 °C, activated carbon with ignition point higher than 400 °C can be prepared. The increase of T_a promotes the aromatic ring structure of activated carbon. This relationship provides a basis for the improvement of structure order and graphitization degree of activated carbon. However, it is unfavorable for the adsorption performance of activated carbon, especially at high T_a.

3. With the increase of T_a, micropores are generated first, followed by mesopores. The V_{mes}/V_{tot} ratio of activated carbon increases with the elevation of T_a and reaches a maximum at 450 °C. The iodine number (IN) and methylene blue number (MBN) of activated carbon are related to micropore volume and mesopore volume, respectively. For preparation of activated carbon with high IN and MBN, the T_a should be between 350 and 425 °C.

ACKNOWLEDGMENTS

REFERENCES CITED

Benaddi, H., Legras, D., Rouzaud, J. N., and Beguin, F. (1998). "Influence of the atmosphere in the chemical activation of wood by phosphoric acid," *Carbon* 36(3), 306-309. DOI: 10.1016/S0008-6223(98)80123-1

Chen, Y., Zhai, S. R., Liu, N., Song, Y., An, Q. D., and Song, X. W. (2013). "Dye removal of activated carbons prepared from NaOH-pretreated rice husks by low-temperature solution-processed carbonization and H_3PO_4 activation," *Bioresource Technology* 144, 401-409. DOI: 10.1016/j.biortech.2013.07.002

Chen, H., Guo, Y. C., Wang, F., Wang, G., and Yu, F. (2017). "An activated carbon derived from tobacco waste for use as a supercapacitor electrode material," *New Carbon Materials* 32(6), 592-599. DOI: 10.1016/S1872-5805(17)60140-9

Chen, D., Gao, A., Cen, K., Zhang, J., Cao, X., and Ma, Z. (2018). "Investigation of biomass torrefaction based on three major components: Hemicellulose, cellulose, and lignin," *Energy Conversion and Management* 169, 228-237. DOI:10.1016/j.enconman.2018.05.063

Demiral, I., and Şamdan, C. A. (2016). "Preparation and characterisation of activated carbon from pumpkin seed shell using H_3PO_4," *Anadolu University Journal of Science and Technology. A: Applied Sciences and Engineering* 17(1), 125-138.DOI: 10.18038/btda.64281

Duan, X. L., Yuan, C. G., Jing, T. T., and Yuan, X. D. (2019). "Removal of elemental mercury using large surface area micro-porous corn cob activated carbon by zinc chloride activation," *Fuel* 239, 830-840. DOI: 10.1016/j.fuel.2018.11.017

Environmental Monitoring Center Station of Ningxia (2018). "Letter on seeking opinions on four national environmental protection standards including 'emission standards of pollutants for activated carbon industry (Draft)'," The Ministry of Environmental Protection of the People's Republic of China, (http://www.mee.gov.cn/gkml/hbb/bgth/201803/t20180315_432536.htm).

Ferrera-Lorenzo, N., Fuente, E., Suárez-Ruiz, I., Gil, R. R., and Ruiz, B. (2014). "Pyrolysis characteristics of a macroalgae solid waste generated by the industrial production of agar-agar," *Journal of Analytical and Applied Pyrolysis* 105, 209-216. DOI: 10.1016/j.jaap.2013.11.006

Foo, P. Y. L., and Lee, L. Y. (2010). "Preparation of activated carbon from *Parkia speciosa* pod by chemical activation," in: *Proceedings of the World Congress on Engineering and Computer Science*, San Francisco, USA, pp. 696-698.

Fu, Y. H., Shen, Y. F., Zhang, Z. D., Ge, X. L., and Chen, M. D. (2019). "Activated bio-chars derived from rice husk *via* one- and two-step KOH-catalyzed pyrolysis for phenol adsorption," *Science of the Total Environment* 646, 1567-1577. DOI: 10.1016/j.scitotenv.2018.07.423

Greenwood, N. N., and Earnshaw, A. (1997). *Chemistry of the Elements*, Butterworth-Heinemann, Oxford, UK.

Heidarinejad, Z., Dehghani, M. H., Heidari, M., Javedan, G., Ali, I., and Sillanpää, M. (2020). "Methods for preparation and activation of activated carbon: A review," *Environmental Chemistry Letters* 18, 393-415. DOI: 10.1007/s10311-019-00955-0

Hesas, R. H., Arami-Niya, A., Wan Daud, W. M. A., and Sahu, J. N. (2013). "Preparation and characterization of activated carbon from apple waste by microwave-assisted phosphoric acid activation: Application in methylene blue adsorption," *BioResources* 8(2), 2950-2966. DOI: 10.15376/biores.8.2.2950-2966

Hirunpraditkoon, S., Srinophakun, P., Sombun, N., and Moore, E. J. (2015). "Synthesis of activated carbon from jatropha seed coat and application to adsorption of iodine and methylene blue," *Chemical Engineering Communications* 202(1), 32-47. DOI: 10.1080/00986445.2013.828611

Ioannidou, O., and Zabaniotou, A. (2007). "Agricultural residues as precursors for activated carbon production – A review," *Renewable and Sustainable Energy Reviews* 11(9), 1966-2005. DOI: 10.1016/j.rser.2006.03.013

Jagtoyen, M., and Derbyshire, F. (1998). "Activated carbons from yellow poplar and white oak by H_3PO_4 activation," *Carbon* 36(7-8), 1085-1097. DOI: 10.1016/S0008-6223(98)00082-7

Jain, A., Balasubramanian, R., and Srinivasan, M. P. (2016). "Hydrothermal conversion of biomass waste to activated carbon with high porosity: A review," *Chemical Engineering Journal* 283, 789-805. DOI: 10.1016/j.cej.2015.08.014

Kang, S. M., Jiang, S. H., Peng, Z. Z., Lu, Y., Guo, J. F., Li, J. W., Zeng, W. X., and Lin, X. Y. (2018). "Valorization of humins by phosphoric acid activation for activated

carbon production," *Biomass Conversion and Biorefinery* 8(4), 889-897. DOI:10.1007/s13399-018-0329-3

Leung, P. S., and Safford, G. J. (1970). "An investigation of the early stage graphitization process by neutron inelastic scattering," *Carbon* 8(4), 527-544. DOI: 10.1016/0008-6223(70)90015-1

Li, Y. X., Zhang, X., Yang, R. G., Li, G. Y., and Hu, C. W. (2015). "The role of H_3PO_4 in the preparation of activated carbon from NaOH-treated rice husk residue," *RSC Advances* 5(41), 32626-32636. DOI: 10.1039/c5ra04634c

Luo, Y. P., Li, D., Chen, Y. C., Sun, X. Y., Cao, Q., and Liu, X. F. (2019). "The performance of phosphoric acid in the preparation of activated carbon-containing phosphorus species from rice husk residue," *Journal of Materials Science* 54(6), 5008-5021. DOI: 10.1007/s10853-018-03220-x

Ma, Z. Q., Wang, J. H., Yang, Y. Y., Zhang, Y., Zhao, C., Yu, Y. M., and Wang, S. R. (2018). "Comparison of the thermal degradation behaviors and kinetics of palm oil waste under nitrogen and air atmosphere in TGA-FTIR with a complementary use of model-free and model-fitting approaches," *Journal of Analytical and Applied Pyrolysis* 134, 12-24. DOI: 10.1016/j.jaap.2018.04.002

Ma, Z. Q., Yang, Y. Y., Ma, Q. Q., Zhou, H. Z., Luo, X. P., Liu, X. H., and Wang, S. R. (2017). "Evolution of the chemical composition, functional group, pore structure and crystallographic structure of bio-char from palm kernel shell pyrolysis under different temperatures," *Journal of Analytical and Applied Pyrolysis* 127, 350-359. DOI: 10.1016/j.jaap.2017.07.015

Malaika, A., Rechnia-Gorący, P., Kot, M., and Kozłowski, M. (2018). "Selective and efficient dimerization of isobutene over H_3PO_4/activated carbon catalysts," *Catalysis Today* 301, 266-273. DOI: 10.1016/j.cattod.2017.02.038

Mao, H., Chen, X., Huang, R., Chen, M., Yang, R., Lan, P., Zhou, M., Zhang, F., Yang, Y., and Zhou, X. (2018). "Fast preparation of carbon spheres from enzymatic hydrolysis lignin: Effects of hydrothermal carbonization conditions," *Scientific Reports* 8(1), 9501. DOI: 10.1038/s41598-018-27777-4

Mao, H., Zhou, D., Hashisho, Z., Wang, S., Chen, H., and Wang, H. (2015). "Preparation of pinewood and wheat straw-based activated carbon via a microwave-assisted potassium hydroxide treatment and an analysis of the effects of the microwave activation conditions," *BioResources* 10(1), 809-821. DOI: 10.15376/biores.10.1.809-821

Mao, H., Tang, J., Xu, J., Peng, Y., Chen, J., Wu, B., Jiang, Y., Hou, K., Chen, S., Wang, J., Lee, H. R., Halat, D. M., Zhang, B., Chen, W., Plantz, A. Z., Lu, Z., Cui, Y., and Reimer, J. A. (2020). "Revealing molecular mechanisms in hierarchical nanoporous carbon via nuclear magnetic resonance," *Matter* 3(6), 2093-2107. DOI: 10.1016/j.matt.2020.09.024

Nunes, C. A., and Guerreiro, M. C. (2011). "Estimation of surface area and pore volume of activated carbons by methylene blue and iodine numbers," *Química Nova* 34(3), 472-476. DOI: 10.1590/S0100-40422011000300020

Olivares-Marín, M., Fernández-González, C., Macías-García, A., and Gómez-Serrano, V. (2006). "Thermal behaviour of lignocellulosic material in the presence of phosphoric acid. Influence of the acid content in the initial solution," *Carbon* 44(11), 2347-2350. DOI: 10.1016/j.carbon.2006.04.004

Puziy, A. M., Poddubnaya, O. I., Martínez-Alonso, A., Suárez-García, F., and Tascón, J. M. (2005). "Surface chemistry of phosphorus-containing carbons of lignocellulosic origin," *Carbon* 43(14), 2857-2868. DOI: 10.1016/j.carbon.2005.06.014

Puziy, A. M., Poddubnaya, O. I., Martínez-Alonso, A., Suárez-García, F., and Tascón, J. M. D. (2002). "Synthetic carbons activated with phosphoric acid: I. Surface chemistry and ion binding properties," *Carbon* 40(9), 1493-1505. DOI: 10.1016/S0008-6223(01)00317-7

Romero-Anaya, A. J., Lillo-Ródenas, M. A., Lecea, C. S. M., and Linares-Solano, A. (2012). "Hydrothermal and conventional H_3PO_4 activation of two natural bio-fibers," *Carbon* 50(9), 3158-3169. DOI: 10.1016/j.carbon.2011.10.031

Rouquerol, J., Avnir, D., Fairbridge, C. W., Everett, D. H., Haynes, J. M., Pernicone, N., Ramsay, J. D. F., Sing, K. S. W., and Unger, K. K. (1994). "Recommendations for the characterization of porous solids," *Pure and Applied Chemistry* 66(8), 1739-1758. DOI: 10.1351/pac199466081739

Sing, K. S. W. (1982). "Reporting physisorption data for gas/solid systems with special reference to the determination of surface area and porosity," *Pure and Applied Chemistry* 54(11), 2201-2218. DOI: 10.1351/pac198557040603

Solum, M. S., Pugmire, R. J., Jagtoyen, M., and Derbyshire, F. (1995). "Evolution of carbon structure in chemically activated wood," *Carbon* 33(9), 1247-1254. DOI: 10.1016/0008-6223(95)00067-N

Suárez-García, F., Martínez-Alonso, A., and Tascón, J. M. (2004). "Activated carbon fibers from Nomex by chemical activation with phosphoric acid," *Carbon* 42(8), 1419-1426. DOI: 10.1016/j.carbon.2003.11.011

Villota, E. M., Lei, H. W., Qian, M., Yang, Z. X., Villota, S. M. A., Zhang, Y. Y., and Yadavalli, G. (2017). "Optimizing microwave-assisted pyrolysis of phosphoric acid-activated biomass: Impact of concentration on heating rate and carbonization time," *ACS Sustainable Chemistry & Engineering* 6(1), 1318-1326. DOI: 10.1021/acssuschemeng.7b03669

Wada, M., Hori, R., Kim, U. J., and Sasaki, S. (2010). "X-ray diffraction study on the thermal expansion behavior of cellulose Iβ and its high-temperature phase," *Polymer Degradation & Stability* 95(8), 1330-1334. DOI: 10.1016/j.polymdegradstab.2010.01.034

Wigmans, T. (1986). *Fundamentals and Practical Implications of Activated Carbon Production by Partial Gasification of Carbonaceous Materials*, Martinus Nijhoff Publishers, Leiden, Netherlands.

Wu, H. F., Chen, R. Y., Du, H. X., Zhang, J., Shi, L. M., Qin, Y., Yue, L. Z., and Wang, J. P. (2019). "Synthesis of activated carbon from peanut shell as dye adsorbents for wastewater treatment," *Adsorption Science & Technology* 37(1-2), 34-48. DOI: 10.1177/0263617418807856

Yagmur, E., Inal, I. I. G., Gokce, Y., Ghobadi, T. G. U., Aktar, T., and Aktas, Z.(2018). "Examination of gas and solid products during the preparation of activated carbon using phosphoric acid," *Journal of Environmental Management* 228, 328-335. DOI: 10.1016/j.jenvman.2018.09.046

Yahya, M. A., Al-Qodah, Z., and Zanariah, N. C. W. (2015). "Agricultural bio-waste materials as potential sustainable precursors used for activated carbon production: A review," *Renewable & Sustainable Energy Review* 46, 218-235. DOI: 10.1016/j.rser.2015.02.051

Yakout, S. M., and Sharaf El-Deen, G. (2011). "Characterization of activated carbon prepared by phosphoric acid activation of olive stones," *Arabian Journal of Chemistry* 9(S2), S1155-S1162. DOI: 10.1016/j.arabjc.2011.12.002

Yang, H., Yan, R., Chen, H., Lee, D., and Zheng, C. (2007). "Characteristics of hemicellulose, cellulose and lignin pyrolysis," *Fuel* 86(12-13), 1781-1788. DOI: 10.1016/j.fuel.2006.12.013

Yorgun, S., and Yildiz, D. (2015). "Preparation and characterization of activated carbons from Paulownia wood by chemical activation with H_3PO_4," *Journal of The Taiwan Institute of Chemical Engineers* 53, 122-131. DOI: 10.1016/j.jtice.2015.02.032

Zuo, S. L. (2018). "A review of the control of pore texture of phosphoric acid-activated carbons," *New Carbon Materials* 33(4), 289-302. DOI: 10.19869/j.ncm.1007-8827.2018.04.001

Zuo, S. L., Yang, J. X., and Liu, J. L. (2010). "Effects of the heating history of impregnated lignocellulosic material on pore development during phosphoric acid activation," *Carbon* 48(11), 3293-3295. DOI: 10.1016/j.carbon.2010.04.042